Title

ANALYSES OF IRON CONTENT IN INDIVIDUAL HUMAN RED BLOOD CELLS BY ELECTRON MICROPROBE AND SCANNING ELECTRON MICROSCOPE

Author

Davis, D.

Publication Date

1977-08-01

Submitted to Journal of Cell Biology

LBL-5636
Preprint

ANALYSES OF IRON CONTENT IN INDIVIDUAL HUMAN RED BLOOD CELLS BY ELECTRON MICROPROBE AND SCANNING ELECTRON MICROSCOPE

David Davis

DONNER LABORATORY

August 1977

Prepared for the U. S. Energy Research and Development Administration under Contract W-7405-ENG-48

DISCLAIMER

ANALYSES OF IRON CONTENT IN INDIVIDUAL HUMAN RED BLOOD CELLS BY ELECTRON MICROPROBE AND SCANNING ELECTRON MICROSCOPE

DAVID DAVIS

From Donner Laboratory, Lawrence Berkeley Laboratory, University of California, Berkeley, California 94720

ABSTRACT

The iron content of single human red blood cells has been assessed using electron microprobe analysis and scanning electron microscopy. Cells for microanalysis consist of a fixed-washed and freeze-dried preparation. This preparative procedure improves stability and spatial resolution of the analytic method. The reference standard employs compressed pellets of purified iron-containing human hemoglobin and human serum albumin, respectively. The cell preparation and reference standard remain stable for long periods of time. Differences in Fe content and its distribution among individual red cells from both normal subjects and sickle cell anemia patients have been measured by the quantitative and semi-quantitative techniques (wavelength and energy dispersive x-ray spectrometry). There are several points which can be made from this study. One concerns the estimates of iron on a cell by cell basis, the average variation among cells being slightly over 13%, ranging from 6% to 19.4% by individuals or by groups from 11% to 14%, these differences thus being closely comparable across ethnic groupings with a possibility of higher level in Asians and

lower level in sickle cell anemia patients. The iron K-radiation frequency distribution curves for both normal and sickle cell groups very closely approximate a normal probability curve.

INTRODUCTION

The distribution of iron among individual red blood cells can give a valuable parameter to add to the well-known average values obtained from multicell analyses. In addition, if subpopulations of cells can be distinguished on a morphological basis, e.g., sickle cell anemia preparation, then the distribution of iron between the subpopulations can only be measured by analyzing individual cells.

This study presents a detailed account of a quantitative and semi-quantitative analyses of bound-iron content of individual red cells by means of analytical procedures utilizing electron probe excitation. The physical instruments whose adaptability and sensitivity were explored are (1) electron microprobe analyzer (EMPA) and (2) scanning electron microscope (SEM) fitted with an energy dispersive x-ray spectrometry (EDX) system. A major emphasis is placed on EMPA because of the broad applications and extensive theoretical development which it has undergone in the past twenty-odd years and personal experience (21,22) in the study and use of this instrument.

The differences in iron content in individual human red blood cells were determined, and the following issues were chosen for investigation:

(1) constancy or variation among circulating erythrocytes of the same population (i.e., same subject);

(2) constancy or variation over a period of time (two weeks) which would represent an appreciable fraction of an individual's erythrocytic turnover (three samples drawn at approximately weekly intervals span 14 days of the 120-day average red cell life);

(3) degree of constancy or variation among different individuals who are presumed "euhemic" based on absence of clinical complaints and on microscopic observation of cell form;

(4) possible alteration in Fe content in a major blood dyscrasia.

The choice of the dyscrasia to be investigated determined a part of the selection of the presumably normal individuals. Sickle cell anemia was chosen, being not only genetically but also ethnically determined and providing erythrocytes with high morphologic recognition. Thus the groups of normal individuals required to be included were not only Blacks (for the sickle cell anemia comparison) but also at least one other ethnic group. In fact, two were tested — Whites and Asians (Chinese).

The Principles of the Analytic Method in EMPA

Each chemical element emits characteristic x-ray lines when it is excited by high energy electrons. By analyzing the wavelengths of the emerging x-ray photons, elements can be identified. By measuring the intensities of the x-ray lines emitted, the amounts of the elements present can be evaluated.

Historical Development of the Theory

The foundation for x-ray spectroscopy was established around the turn of this century (18). Methods for x-ray production by means of electron excitation came two decades later. One of the first studies to make use of the electron microanalysis soon followed, but this method of analysis did not spread until Castaing, in his Ph.D. thesis led by A. Guinier, laid the practical and theoretical foundation for x-ray microanalysis (5). Since that time, Mulvey had built a static microanalyzer and added in 1956 the scanning mode of operation (19) which Cosslett developed independently (6). The instrument grew out of the marriage of two technologies, x-ray fluorescence spectroscopy and electron microscopy. The first biological applications were on bulk-hard samples – bone (3) and teeth (2). The electron microprobe, as we know it today, has come to be thought of as a powerful tool for biologists.

MATERIALS AND METHODS

Elemental Analysis

Two instruments were used in measuring the iron content in single human red blood cells:

(a) a Materials Analysis Company (Palo Alto, California) electron microprobe analyzer, Model 400S, operated at 15 keV with a 1.2 to 2.0 μm beam diameter with a sample current of 0.05 – 0.07 μA, and a LiF analyzing crystal for Fe and a PET crystal for Si;

(b) a Japan Electron Optics Laboratory (Burlingame, California) scanning electron microscope, Model Uℓ operated at 15 keV at a magnification of X50,000 with T.V. rates, interfaced with a Nuclear Equipment Corporation (Los Altos, California) solid-state detector and Qanta/Metrix (Sunnyvale, California) EDX/80S energy dispersive x-ray analysis system.

Cells

Human circulating erythrocytes were obtained from normal subjects and sickle cell anemia patients. The latter were collected fresh into heparinized syringes and prepared for analysis within 24 hours of collection; the former was collected by conventional finger-puncture method. This blood was prepared in the following manner: a single drop of blood was placed directly onto the surface of a three-inch parafilm square that was immediately inverted over the mouth of an Ehrlenmeyer flask containing 50 ml of a 2.5% glutaldehyde solution in 0.15 M cacodylate buffer at pH 7.4. The edges of the square were pressed down securely and held by hand around the neck of the flask so as to render it liquid-tight; and the cells were then mixed by gentle, repeated inversions of the flask enough times until visual observation had confirmed thorough dispersion in the fixative. After 45 minutes to an hour fixation time, the cells were washed; and a ml portion of the fixed cell suspension was spun down in a

table model IEC clinical centrifuge at about 5,000 rpms for three minutes. The supernate was discarded, and the remaining cells were resuspended in a ml of distilled water and centrifuged. This suspension and centrifugation procedure was repeated three times. After this wash procedure, the cells were resuspended in 1/2 ml to 1 ml of water to which a very small amount (approximately one µg/cc) of scientific grade gelatin (Difco) had been added. These resuspended cells were then mounted on top of a quartz disk by transferring about 1/8 ml to 1/4 ml of suspension drop by drop with a disposable pipette, the total number of drops having been determined by the size of the counting area desired such that this area did not exceed the size of the disk in order to avoid spillage. After allowing the cells to settle for 15 minutes, the excess water was drawn off by capillary action, using a corner of a gauze square. This preparation was quenched in liquid nitrogen, before it dried, to effect rapid-freezing and was transferred to a pre-cooled castle (a specially constructed, aluminum lidded container for freeze-drying biological materials). After securing the lid, the castle was quickly placed onto the pre-cooled stage in an Edwards-Pearse Tissue Dryer, Model EPD2, (Edwards High Vacuum, Inc., Grand Island, N.Y.) equipped with a liquid nitrogen trap fitted into the pumping line, and dried under vacuum for 24 to 48 hours at -60°C with a P_2O_5 desiccant present in the drying chamber; the pressure drop in the specimen chamber indicates that the preparation has dried. This freeze-dried preparation was slowly heated to room temperature for removal from the drying chamber, then put into a Varian Evaporator (Varian Associates, Palo Alto, California), Model Ve-10, equipped with a liquid nitrogen cold trap in a pumping line, and coated with carbon to improve conduction and reduce charging. During coating, the sample revolved simultaneously in opposite directions in two different planes. Though the thickness of the carbon coating was not determined, the amount was established and controlled by evaporating the 3/16-in. long tip of a pre-sharpened

spectroscopically pure carbon rod onto the sample. The preparation, ready for analysis, was stored in a desiccator jar under vacuum.

Reference Standard

The standards used for analysis were pellets pressed from purified powders of human hemoglobin (Hb) and serum albumin (Alb). These were prepared by placing about 5 to 10 mg of granulated, spectroscopic grade carbon into the bore of a mold-plunger assembly. The plunger was put into place, and the carbon was packed tightly by hand pressure only. The plunger was withdrawn, and 40 mg of Hb was poured on top of the carbon through the bore of the mold. The plunger was again replaced, and the mold-plunger assembly was put into a vacuum unit which permitted the application of mechanical pressure while under vacuum. A Black Hawk Hydraulic Press (Black Hawk Collision and Repair Div., Milwaukee, Wisconsin) applied 3,000 to 4,000 psi to the Hb, forming a disk-shaped pellet 1/4-in. in diameter. After about three to five minutes, the mechanically applied pressure was released and the vacuum was removed. The mold-assembly was then taken from the vacuum unit, and the Hb pellet was carefully removed from the mold. This same procedure was repeated with the Alb. The Hb and Alb pellets thus obtained were mounted next to each other in the center of the quartz disk (Fig. 1) with colloidal graphite in alcohol (Dag, Acheson Colloids Co., Port Huron, Michigan). This standard reference preparation was carbon-coated along with the cell preparations described in the previous section.

EMPA

In the electron microprobe, analysis was performed on each erythrocyte while under visual observation. The cell was counted for a total of five minutes (in five 1-minute intervals). Two elements (Fe and Si) were analyzed simultaneously. The x-ray backgrounds were measured in noncell areas of the

supporting quartz disk with the spectrometers held in their respective peaks. Probe standards, pure Fe and SiO_2 were used to maintain similar probe conditions from experiment to experiment and for probe stability checks. Intensities of the probe standard and reference standards and their respective backgrounds were measured before each series of ten cells.

The relative concentration values in the red cells were estimated by using the average value of the net intensity of the cells in conjunction with net intensity values and known concentrations of the reference standard as provided by this mathematical relationship: $C_c = I_c/I_s \times C_s$ where C_c is the relative mean iron concentration in the rbc; C_s is the known average iron concentration value of the reference standard in weight per cent (i.e., g/100g), I_c is the mean net Fe K_a intensity obtained from an rbc, and I_s is the mean net Fe K_a intensity obtained from the standard. The concentration values calculated in this manner were not corrected for ZAF differences between the sample and the standard since these effects should have been small due to the similarity between the cell and the reference standard in composition and nature of matrix.

The detection sensitivity of the EMPA was computed according to the equation of Liebhafsky et al. (14). In addition to the three sigma computation above, a 95% confidence interval was also computed.

SEM-EDX

In the scanning electron microscope, selected post-EMPA and thin film (Formvar) preparations were examined in the secondary electron image and x-ray modes. The images were recorded by making a 40 and 70 sec scan. Energy dispersive x-ray spectra were obtained by using an attached liquid nitrogen-cooled Li-drifted-Si semiconductor x-ray detector, operating at an accelerating voltage of 15 keV, beam current 10^{-9} to 10^{-10}A, and a takeoff angle of 45^{o}. The condenser lens and scan oil settings were maintained at a constant setting.

Estimates of Fe K-radiation per cell were obtained under the same SEM operating conditions as those for the plotted spectra except for the x-ray count rate integration periods (e.g., five 1-minute intervals for computed runs). Subtraction of background and integration of remaining peaks of the x-ray data were obtained automatically by a coupled mini-computer interfaced with the scaler of the SEM x-ray detector. The print-out was recorded by an ASR-33 teletype and spectra plots were recorded by an X-Y input-output plotter.

RESULTS

Elemental Analysis

The selection of the proper computer program for quantitation of the EMPA intensity data was a difficult matter because of the nature of biological specimens. One should take into account also their thickness. The computer routine used was DATATEXT, a general one, designed for the behavioral sciences to perform basic statistics and ANOVA. The advantage of the use of such a scheme is low cost and availability of a computer center for batch loading of IBM card file data. Large quantities of data can be run in seconds for under $10 at current rates.

Whole Blood Preparation

A preliminary experiment was carried out with air-dried whole blood smears employed as the sample preparation for EMPA. This seemingly ideal specimen preparation from the point of view of minimizing iron loss proved to be most undesirable for the following reasons: significantly higher mean background x-ray signals; corresponding low signal intensities from the cells; and, more importantly, a relative increase in the electrical instability (charging) of the sample itself. Lechene (13) reported similar problems when EMPA was performed on a specimen preparation of the same type as above. Figures 2a, b, and c show examples of the mentioned preparation. In Fig. 2b, salt crystals (mostly sodium) and flattened, shrunken cells can be clearly seen (Fig. 2c) which shows cracks encircling cells' periphery at high magnification. This surface discontinuity contributes to sample instability, i.e., a charging artifact that is denoted by the peripheral halo seen at all magnifications.

Sample Stability and Durability

Standard deviation of the mean was obtained through manual calculations as well in order to detect variation in multiple readings on the same cell and, in particular, to look for systematic change in successive readings which would reflect deterioration of the sample by the beam.

Table I, showing sample stability and durability under analysis, yields the following conclusions:

(1) variation among successive readings on the same cell or pellet (reference standard) sample is random and small within limits of acceptability for statistical comparisons of samples;

(2) no significant degradation of the cell under probe took place during successive readings;

(3) in terms of stability of cell preparation, there was no measurable instability when analysis time was extended threefold.

Characteristics of Background (N_B)

Two considerations entered examining N_B traits: to determine N_B as affected by the support — SiO_2, i.e., the inseparable Bremsstrahlung and environmental sources; and the other was the organic matrix Alb, e.g., signal specificity.

The data in Table II — Characteristics of Background (N_B) — can be summarized as follows:

(1) the support and the preparative procedures and milieu yield a background so low as not to obscure the N_L derived from the analyses;

(2) the protein pellet has similarly low nonspecific values; and

(3) the pellet provides the better background characteristic.

Energy Operating Potential

To determine the optimal instrumental applied potential, a sufficiently broad range was tested.

Table III, which indicates choice of energy operating potential (i.e., 15 keV), shows the maximal and minimal levels and the intermediate level selected as optimal for use. These results were based on actual measurement of low Fe concentration in single cells.

Constancy of Cell Population

Findings on circulating erythrocytes of the same blood sample were determined from normal subjects. In each normal subject, the sample was divided among three disks. Ten cells were measured on each disk. Values were determined from five points on each cell (in cpm). Table IV, neatly condensing the experimental design, shows the distribution of ethnic and related groups.

It was concluded that the average variation among cells on the same disk was slightly over 13%, ranging from 6% to 19.4%. When considered by individuals or by groups, the average variation was encountered among groups (11% to 14%), thus giving added confidence to the objective of studying ethnic and related groups; the initial analysis was done without ethnic group breakdown (Tables IV a, b, c).

Effects of Time Lapse in Sampling Sequence

The possible variation over a two-week period was examined by breaking up the foregoing determinations on normal subjects into data from the three successive samplings in that time period (see Table V). The effects of time of

sampling were minor and followed no systematic change for differences among mean readings yielded in the time period specified.

Constancy — Cells of Normal Subjects and Sickle Cell Anemia Patients

Table VI, the statistical treatment of data, defines well the constancy among cells of normal subjects and sickle cell anemia patients; this data, when viewed by disk, revealed no significant difference between the groups. Inspection of the ranges and standard error of the data shown yields the following conclusions and suggestions:

(1) there was no significant difference in the Fe K_a total intensities from the sickle cell samples and full complement of normal cell samples;

(2) normal cell samples from Asians (top three sets in Table VI) tended to run appreciably higher than similar samples from Blacks and Whites; the latter two groups (middle and lower euhemic sets were essentially similar);

(3) the suggestion of somewhat high iron concentration in Asian erythrocytes (at least among subjects used in this study) became stronger when analyses of the three disks per person were combined into figures representing individual subjects; under these circumstances there was no overlap between the lower values in Blacks and high values in Asians, and only slight overlap between Whites and Asians;

(4) continuing to treat the data from individual subjects, the Black normal and Black sickle cell groups were virtually identical.

Thus, with all necessary reservation regarding the adequacy of sampling numbers in the various groups, it appears that the average iron content of red cells and its distribution among individual red cells is closely comparable across ethnic groupings (with a possibility of higher level in Asians);

furthermore, in the blood dyscrasia chosen (sickle cell anemia) the iron content of individual cells remains within the normal range.

Relative Frequency Distribution of Fe K_a Net Intensity in Human rbc's

The distribution of the iron values in the two populations of cells measured was computed as the relative frequency of each of the values encountered (Table VII) and plotted as a histogram (Fig. 10). It should be emphasized that these counting rates are net values, i.e., above background. The resultant curve for the cell population (i.e., 300 red cells) showed a very close approximation to the normal probability. The values from the sickle cell anemia samples are added (shown stippled in the histogram). While the sample is small, leaving many open classes, the frequency distribution confirms foregoing conclusions, namely, that the greatest frequencies are found somewhat lower in the scale but are still grouped according to a normal probability distribution.

Scanning Electron Microscopy

Secondary Electron Examination

Some examples selected from many samples studied are presented below to illustrate the potential capabilities that this analytical system, i.e., secondary and EDX modes, affords the biologist.

The SEM micrograph (Fig.11a) shows a typical morphology of a euhemic human red blood cell. Although this cell consisted largely of water (65%), it tends to maintain more of its overall morphology by this preparative method, although the filamentous aggregate, as an artifact, leaves something to be desired (seen in Fig.11b).

Figure 12 shows the cellular morphology of a sickle cell anemia blood sample. This micrograph illustrates two images, one sickled (echinocyte) and one normal-appearing (discocyte) as identified by Ponder (20).

Figure 3 micrographically illustrates the morphology of red cells as they appear after being prepared in a manner similar to the above red cells mounted on SiO_2 except that these are mounted on a thin film, allowed to air dry, and examined without the addition of any conductive coating materials. There are signs of cellular collapse (flattening) and these cells are somewhat distorted.

Figure 4 shows SEM micrographs in three-dimensional presentation (stereo-pairs technique) of the above samples. It is shown here depicting vertical display [Nesch Vertical System after Mannheim, (16)]. This technique eliminates the problems of convergence, interocular distance, and picture size.

Figure 5 illustrates the use of finder grids (alphabetized) for x-ray spectrometry in the SEM (or EMPA). Thus, single cells are selected by SEM imaging. The pre-analysis micrograph is made; then x-ray spectrometry is performed, etc., and postanalysis micrographs can be accomplished of said cells.

EDX Analysis

A scanning electron microscope—energy dispersive system for the semi-qualitative analysis of purified human hemoglobin and human serum albumin (i.e., the reference standard)—was used in forming the spectrum shown in Fig. 6. The spectrum, representing the x-ray energies for first quarter of the Periodic Table has prominent peaks for Si and S, and also well-defined peaks for Cl, K, and Fe.

Figure 7 is the spectrum representing the x-ray analysis of a single human rbc mounted on SiO_2 and the corresponding off cell analysis; this spectrum has a strong peak for Si with well-defined Fe and Cu peaks as well; Si measurement is against a very high continuous radiation background reflecting the high excitation rate of Si. The Cu peak is present in both on cell and off cell spectra and probably represents the copper parts of the instrument as a remote source.

Figure 8 shows the spectrum representing the analysis of a single human rbc mounted on thin film. The K_a x-ray lines of Fe, Cu, S, Cl, Si, and Al are shown. Iron and sulfur are shown as prominent cell components. Background continuous radiation count has been reduced to 20% of the value when the cell was analyzed on the quartz disk mount. The large Cu peak is due to the supporting copper grid.

Figure 9 illustrates the typical Fe K_a x-ray lines of the x-ray energies for a single human rbc mounted on a quartz disk compared to one mounted on thin film (isolated peaks); the adverse affect of a very high continuous radiation background is explicit.

Data Reduction

X-ray counts for Fe were also made for a series of ten euhemic red cells. Table VIII gives the statistical treatment of the mean total x-ray intensity value for each cell and for the white radiation. It was concluded from the statistical treatment of these data that the average variation among cells was a little more than 21% and ranged from a low of 1% to a high of 85%. When an estimated variation for the corresponding off cell analyses on the same sample is being considered, this average value is slightly over 1% less than the variation obtained from the on cell analyses; however, the grand mean for the N_T value in this case is 5% higher than the latter.

The results of the x-ray counts from a blood sample from a sickle cell anemia patient, arranged by cell morphology (sickle and normal-appearing cells), are seen in Table IX. This analysis yielded similar conclusions when compared with the data above.

Table X shows the analyses of eight euhemic cell types mounted on thin film. The conclusions drawn from these trials are: (1) the thin film support effected a substantial decrease in the N_B intensity; (2) N_T showed a corresponding reduction; and (3) the N_T/N_B intensities were not significantly improved by this approach.

DISCUSSION

The subject of x-ray spectrometry, as employed by the EMPA system according to Bragg's Law and as utilized by SEM-EDX system according to Moseley's Law, is well established; and information obtained from either system is qualitatively the same; however, detection limits impose certain restraints on their resolution if comparisons are to be made.

In practice, then, there are of interest important drawbacks that have become evident through the use of EDS in EMPA and SEM systems in biological studies: increased background signal; serious energy interferences at low x-ray energy; x-ray sources remote from the specimen (backscattered electrons from the specimen generate x-rays indiscriminately upon striking any object inside the specimen chamber as well as the chamber wall); low peak-to-background ratios (P/B). It is important to note that while a rather convincing argument can be made against the use of P/B because they may not tell the whole story in a direct comparison of WDS and EDS systems, the fact remains, nevertheless, that intensity or P/B data are essential to the quantitative aspects of x-ray microanalysis (11).

Noteworthy are the previous studies (WDS and EDS in EMPA) in which accuracy was the utmost concern in WDS systems, and speed and greater spectrometer sensitivity were the prime motivation in EDS systems. Lechene (13) routinely observed a P/B of 50 from his EMPA of 160 mM Na/kg wet weight, while Dorge and associates (8) reported a low P/B of approximately 0.3 in studying Na in frog skin as a calibration curve on comparable samples when using EDS on the same standard samples as Lechene above. The EMPA permitted the better resolution. The work reported here extends this kind of a study by directly examining the Fe content within individual human rbc's when the average P/B was on the order of 2.2:1 for the Fe analyses, while on the SEM-EDX system the

analyses of the post-EMPA samples were 1.2:1 at best. The two above x-ray spectrometry systems have been described (1).

Limits on energy resolution in the EDS impose restraints on the EDS. For example, Lechene reported using WDS to obtain an energy resolution smaller than 10 eV at 5.9 keV whereas the EDS detection at best will have a resolution of about 142 at 5.9 keV as measured by Hayes and Pawley (12) for MnK_a. In practice this means that the WDS may differentiate between Mg and Na while the EDS system may not. It has been reported that almost all commercially available EDS systems cannot resolve peaks of adjacent elements in the range Be to Na. Reports of EDS analyses reflect the peak overlaps of Ca and Sb because of low concentrations of the elements of interest (25, 24), although such overlaps could easily have been recognized with WDS. As another example, Sutfin et al. (26) demonstrated Os interference with P. Further, there are reported examples of other problems that can arise with EDS: escape peaks (extraneous x-ray peaks that appear in the spectrum and are related to the efficiency of a particular detector); pulse pile-up (summation of two or more x-rays entering the detector very close together in time; an electronic method of rejecting pulse pile-up is currently available); lack of discrimination as to x-ray source in particular peaks originating from outside the analyzed volume and due to backscattered electrons (4, 17). These problems are of special significance when measuring light elements, e.g., $11 \leqslant Z \leqslant 20$, because of x-ray absorption in the detector window (usually beryllium sheet approximately 10 μ thick) and in the lithium-drifted-silicon chip itself; due to such hindrances, these elements are not usually identified or analyzed by means of energy dispersion (10). The performance of the WDS x-ray system in the EMPA and SEM as well is superior in the ability to detect light elements (important ones in biology are C, O, N, and F in dentistry).

Comparative performance of the systems (WDS and EDS in SEM) is considered below. In SEM applications, WDS systems are generally capable of much better resolution than EDS systems; in the latter case a count rate limitation places restraints on its resolving capacity. Woldseth (29) suggested that under this condition decreased resolution is due to pulse pile-up in the detector.

Detectability limits and mass sensitivity are highly controversial subjects in the literature and at scientific meetings. It has been found that calculated limits of detectability for EDS and WDS systems depend as well, among other things, on beam current and matrix. When comparisons are made between the two systems, values of P^2/B are usually considered because sensitivity of an analysis is calculated in terms of weight-fraction or in terms of the absolute quantity; both require peak quantity and background quantity. The use of these values alone can be deceptive (15).

In practice, the intrinsic counting rate limitation for EDS systems increases the difficulty of accurately measuring the small P/B differences (typically associated with elements in low concentration). Spectra interferences (peak overlap) also become troublesome.

In terms of the sensitivity of the above technique, the author's value for minimum detectable limits (MDL) calculated from the SEM-EDX data was 0.19% corresponding to a 95% confidence interval of 0.15 to 0.53% for the Fe value of the rbc (0.34%). However, the experimental intensity data were found to be low: in evidence is a small peak superimposed over a huge background (see Fig. 9). Routinely, the calculated low detectability limits in EDS systems have, in practice, not been found to be applicable to a broad range of SEM studies because of the aforementioned intrinsic difficulties. In this regard, EDS systems seldom perform to their theoretical capabilities except in x-ray fluorescence applications (which are not subjected to the many restrictions of SEM applications). The MDL estimate for EMPA was computed in a similar manner:

first, for the reference standard and second, for the cell on quartz. It was found to be, respectively, 0.02% (a 95% confidence interval ranging from 0.32 to 0.36%) and 0.11% (a range of 0.23 to 0.45%). In cellular analysis, a decrease in sensitivity equivalent to over fivefold when compared to the MDL using the conditions of the reference standard. Under these conditions of EMPA, the intensity data support the calculated minimum detectable concentrations measured experimentally. Therefore, in terms of quantitative analysis, better resolution makes the WDS systems far superior, especially for low concentrations and chemically complex matrices. The results of the analyses shown in Table XI clearly demonstrate the contention that the cause of the general quantitative inaccuracy of the EDS relative to the WDS is directly related to P/B's and the resolution differences of the two instruments. The table also illustrates that the P/B for the SEM application is a factor of two higher for the WDS (i.e., better sensitivity). The low P/B for EDS becomes especially critical when considerations of peak minus background are made.

In this study, the relative iron concentration values computed in this manner are low. Each mean red cell value represents according to estimates obtained from multi-cell analyses, an iron content of 0.34% of hemoglobin [which constitutes 95% of the dry cell weight corresponding to about 10^{-13} g, the absolute value calculated for iron per rbc — based on 3×10^8 molecules as the mean hemoglobin corpuscular concentration by Wintrobe (28)]. In this connection the relative standing of the iron determinations obtained in this present study is somewhat improved. While the determinations have been obtained from single cells analyses, other measurements by multicellular analyses are available. Those of wet chemistry, absorption spectrophotometry are: Dowen (9) reported 0.34 mg l^{-1} red cell concentration calculated from blood to plasma (blood, 0.27 mg l^{-1}; plasma, 0.043 mg l^{-1} g); Delves et al. (7) 381×10^2 mg per 100 mg

and also correlated lowered concentration of iron in whole blood samples with blood pathology (e.g., in anemia); and Schroeder and Nason (23) iron estimates were reported in terms of mg total body blood, plasma, and rbc in reference man: 2,500, 3.6, and 2,400, respectively, with 70.5% in hemoglobin. The latter indicative of a mean corpuscular hemoglobin concentration of 30% [found over four decades ago by Wintrobe, (27)].

In addition, the EDS is sensitive to extraneous x-rays impinging on the detector from widely varying directions and sources (e.g., excited from remote areas by backscattered electrons; from instrument components; from transmission grids; and from secondary excitation of remote sample region). Figures 7 and 8 show examples of this feature of the EDS. The prominent Cu peaks seen in both spectra have their origin outside the analyzing volume. The copper x-rays are from parts of the instrument, thin film, supporting copper grid, respectively.

This situation in the case of the WDS-EMPA is not possible due to the restraints imposed on this system by Bragg's Law by which the WDS is sensitive only to x-rays originating from a point source that has a precise location on the Rowland Circle. Collimation further reduces the contribution of extraneous x-ray signals seen in the SEM-EDS data. The WDS, because of its capabilities — high spectral resolution, low concentration, and light element detectability — offers the major overall advantages favoring x-ray spectrometry of biological materials.

The author would like to thank Professor Thomas L. Hayes for his immeasurable counseling throughout the course of this study and Professor Richard Falk for providing the Qanta/Metrix 80S unit for stages of the work; and to acknowledge the assistance of Mr. David Eaglesfield for computer user's aid and the use of Harvard Computing Center, Cambridge, Mass.

This work was submitted to the Faculty of the University of California at Berkeley in partial satisfaction of the requirement for the Ph.D on December 10, 1976. The work was supported in part by the U.S. Energy Research and Development Administration, by the Associated Western Universities, Inc., by the Graduate Minority Program of the University of California, and by a grant from the National Science Foundation.

REFERENCES

1. Beaman, D. R., and J. A. Isasi. 1971. Electron beam microanalysis Part I — The fundamentals and applications. Mater. Res. Stand. 11:8.

2. Boyde, A., V. R. Switsur and R. W. Fearnhead. 1961. Application of the scanning electron probe microanalyzer to dental tissue. J. Ultrastruct. Res. 5:201.

3. Brooks, E. J., A. J. Tousimis and L. S. Birks. 1962. The distribution of Ca in the epiphyseal cartilage of the rat tibia measured with the electron probe x-ray microanalyzer. J. Ultrastruct. Res. 7:56.

4. Brown, A. M., P. S. Baur and F. H. Tuley. 1975. Phototransduction in aphysia neurons: calcium release from pigmented granules is essential. Science 188:157.

5. Castaing, R. 1951. Application des Sondes Electroniques a Une Methode d'Analyse Ponctuelle Chimique et Cristallographique. Ph.D. thesis, ONERA publication 55, University of Paris, 92 pp.

6. Cosslett, V. E., and P. Duncumb. 1956. Electron microscopy. Proc. Stockholm Conf. Almquist and Wiksell, Stockholm, p. 120.

7. Delves, H. T., G. Shepherd and P. Vinter. 1971. Determination of eleven metals in small samples of blood by sequential solvent extraction and atomic-absorption spectrophotometry. Analyst 96:260.

8. Dorge, A., K. Gehring, W. Nagel and K. Thurav. 1974. Localization of sodium in frog skin by electron microprobe analysis. Arch. Pharmacol. 281:271.

9. Dowen, H. J. M. 1966. Trace Elements in Biochemistry. Academic Press, New York, p. 159.

10. Elad, E., and D. A. Gedcke. 1972. Light element analysis with Si (Li) x-ray energy analyzer. In: Proc. Sixth Internat. Conf. on X-ray Optics and Microanalysis, eds. G. Shinoda, K. Kohra, and T. Ichinokawa. University of Tokyo, Japan, p. 263.

11. Goldstein, J. I. and H. Yakowitz. 1975. Practical Scanning Electron Microscopy. Plenum, New York, 582 pp.

12. Hayes, T. L. and J. B. Pawley. 1976. Private communication.

13. Lechene, C. and R. R. Werner. 1976. Private communication with Laboratory. Ultramicroanalysis x-ray spectrometry by electron probe excitation. To be submitted for publication, Ann. Rev. of Biophys. and Biochem. 1977.

14. Leibhafsky, H. A., H. G. Pfeiffer and P. D. Zemany. 1960. X-ray Microscopy and Microanalysis. Elsevier, New York, p. 321.

15. Lifshin, E. and M. F. Ciccarelli. 1973. Present trends in x-ray analysis with the SEM. Proc. Sixth Ann. IITRI SEM Symp., ed. Om Johari. Chicago, Ill., p. 89.

16. Mannheim, L. A. 1971. Stereoscopic system for any size picture pairs (Nasch Vertical System). Photographic Applications in Sci., Technol. and Med. November, p. 38.

17. Moreton, R. B., P. Echlin, B. L. Gupta, T. A. Hall and T. Weis-Fugh. 1974. Preparation of frozen hydrated tissue sections for x-ray microanalysis in the scanning electron microscope. Nature 247:113.

18. Moseley, H. 1913. The high-frequency spectra of the elements. Philosophical Magazine, 26:1024.

19. Mulvey, T. 1958. Transactions, 4th Int. Conf. on Electron Microscopy, p. 263.

20. Ponder, E. 1948. Hemolysis and Related Phenomena. Grune and Stratton, New York, 311 pp.

21. Robison, W. L. and D. Davis. 1969. Determination of iodine concentration and distribution in rat thyroid follicles by electron-probe microanalysis. J. Cell. Biol. 43:115.

22. Robison, W. L., L. Van Middlesworth and D. Davis. 1971. Calcium, iodine, and phosphorus distribution in human thyroid glands by electron-probe microanalysis. J. Clin. Endocrinol. Metab. 32:786.

23. Schroeder, H. A. and A. P. Nason. 1971. Trace-element analysis in clinical chemistry. Clin. Chem. 17:461.

24. Seatersdal, T. S., R. Myklebust and N. P. Berg Justesen. 1974. Ultrastructural localization of calcium in the pigeon papillary muscle as demonstrated by cytochemical studies and x-ray microanalysis. Cell Tiss. Res. 155:57.

25. Stoeckel, M. E., C. Hindelang-Gertner, H. D. Dellman, A. Porte and F. Statinsky. 1975. Subcellular localization of calcium in the mouse hypophysis. Cell. Tiss. Res. 157:307.

26. Sutfin, L. V., M. E. Hotrop and R. E. Ogilvie. 1971. Microanalysis of individual mitochondrial granules with diameter less than 100 angstroms. Science 174:947.

27. Wintrobe, M. M. 1932. The size and content of the erythrocyte. J. Lab. Clin. Med. 17:899.

28. Wintrobe, M. M. 1967. Clinical Hematology. Sixth edition. Len and Febiger, Philadelphia, Pa.

29. Woldseth, R. 1973. Everything You Always Wanted to Know about X-Ray Energy Spectrometry. Kevex Corp., Burlingame, California.

Table I

Interaction of Beam with Sample
("Durability" Tests)

Series	N_T †	N_L ††
I. Human hemoglobin (pressed powder pellets)	372	343
	355	307
	347	311
10 tests	369	330
	359	325
	365	325
	372	346
	367	331
	353	314
	354	313
II. Same cell	95	20
	103	30
15 tests as follows:	102	32
	105	34
10 tests	100	25
	98	-
	105	-
	108	-
	109	-
	112	-
30-minute interval		
5 tests	95	-
	103	-
	107	-
	136	-
	82	-

† N_T = total intensity (i.e., peak of the Fe K_a lines in cpm).

†† N_L = net intensity (= corrected for total background contributions by subtraction of N_B).

Table II

Magnitude of Background Contributions

Nature of N_B tested*	Standardization runs	
	Grand mean† (normal)	Grand mean† (sickle cell)
Support (SiO_2)	65.584 ± 4.0	62.007 ± 11
Protein pellet (human serum albumin)**	43.351 ± 2.6	46.800 ± 8.5

(See Protocol Appendix B)

*Backgrounds tested at time of running normal and sickle cell preparations.

**See "Materials and Methods" section.

†Means are unweighted averages of cell means.

Table III

Sensitivity at Different Accelerating Potentials

Accelerating potential tested	Intensity readings (N_T from cell*)	N_B	N_T/N_B**
10 KeV	80 68 81 53 48	$\overline{52}$	1.269
15 KeV	183 163 188 227 212	$\overline{65}$	2.994
18 KeV	172 199 222 258 209	$\overline{132}$	1.606

*Nature specified in "Materials and Methods" section.

**Peak-to-background ratio.

Table IV

Experimental Design

Group	Number per group	Category	Number of cells per subject	Total number of cells
A	3	Asian	30	90
B	3	Black	30	90
W	3	White	30	90
B(S)	3	Sickled	10	30
Total number of cells analyzed = 300				

Table IV-a

EMPA

Protocol of Computer Basic Statistics, N_T,

Grouped by Disk (for Euhemic Cells Only), Person, and Group

Disk

Disk number	Mean	SD	V*	N	Variance $(SD)^2$
1	135.900	14.209	10.46	10	201.897
2	152.020	12.658	8.33	10	160.226
3	138.940	10.082	7.27	10	101.651
4	177.000	34.343	19.40	10	1179.459
5	147.620	12.583	8.52	10	158.321
6	134.320	12.301	9.16	10	151.321
7	138.640	11.475	8.28	10	131.607
8	156.380	13.043	8.34	10	170.117
9	149.700	14.055	9.39	10	197.545
10	124.000	8.429	6.80	10	71.056
11	137.200	24.049	17.53	10	578.374
12	128.460	10.632	8.28	10	113.032
13	140.900	10.881	7.70	10	118.393
14	134.600	13.253	9.85	10	175.641
15	131.080	15.581	11.89	10	242.764
16	131.800	13.363	10.14	10	178.567
17	126.080	9.040	7.17	10	81.727
18	131.040	11.004	8.40	10	121.084
19	117.060	11.075	9.46	10	122.651
20	135.720	8.610	6.34	10	74.140
21	132.140	11.483	8.69	10	131.855
22	130.340	7.854	6.03	10	61.687
23	132.940	14.938	11.24	10	223.134
24	143.300	14.748	10.24	10	217.507
25	150.360	14.554	9.68	10	211.833
26	143.180	12.866	8.95	10	165.527
27	129.000	12.772	9.90	10	163.113
	138.138	18.503	13.39	270	342.344

*Pearson's Coefficient of Variation.

Table IV-b

Person

Cell type	Person number	Mean	SD	V	N	Variance $(SD)^2$
Euhemic	1	142.287	14.265	10.03	30	203.491
	2	152.980	28.536	18.65	30	814.329
	3	148.240	14.831	10.00	30	219.955
	4	129.887	16.858	12.99	30	284.207
	5	135.527	13.980	10.32	30	195.429
	6	129.640	11.557	8.91	30	133.556
	7	128.307	13.226	10.31	30	174.923
	8	135.527	14.099	10.40	30	198.782
	9	140.847	16.091	11.42	30	258.917
Sickle	10	137.240	21.211	15.46	10	449.911
	11	122.020	17.934	14.70	10	321.620
	12	131.900	10.962	8.31	10	120.166
		137.363	18.634	13.57	300	347.212

Table IV-c

Group

Group	Mean	SD	V	N	Variance $(SD)^2$
A	147.835	20.778	14.05	90	431.729
B	131.684	14.553	11.05	90	211.785
W	134.893	15.404	11.42	90	237.283
B(S)	130.387	18.357	14.09	30	336.978
	137.363	18.634	13.57	300	347.210

Table V

Effects of Time Lapse in Sampling Sequences
Among Asian Subjects

Week	Subject sample	Mean, N_T	SD	V	$(SD)^2$	N
I	A	135.900	14.209 ± 4.5	10.45	201.897	10
	B	177.000	34.343 ± 11	9.40	101.651	10
	C	138.640	11.475 ± 4.6	8.28	131.667	10
II	A	152.020	12.658 ± 4	8.33	160.226	10
	B	147.620	12.583 ± 4	8.52	158.321	10
	C	156.380	13.043 ± 4	8.34	170.117	10
III	A	138.940	10.082 ± 3	7.26	101.651	10
	B	134.320	12.301 ± 4	9.16	151.321	10
	C	149.700	14.055 ± 4	9.39	197.545	10

Table VI

Net Intensity (N_L) Values—
Corrected for SiO_2 Background

Group	Disk	Means	
		Person	Group
Euhemic	72.500		
	71.020	73.4	
	76.740		
	116.800		
	79.420	89.1	80.524
	71.120		
	79.640		
	83.180	80.0	
	77.300		
	62.800		
	67.800	65.0	
	64.380		
	73.900		
	72.140	69.9	67.140
	63.720		
	68.200		
	64.880	66.5	
	66.440		
	58.689		
	67.320	65.3	
	69.760		
	64.260		
	68.140	68.0	70.060
	71.700		------
			72.577
	89.760		
	76.780	76.9	
	69.200		
Sickle	78.140	78.140	
	58.900	58.900	68.380
	68.100	68.100	------
			72.113

Table VII

Relative Frequency Distribution of Fe K_a Net Intensity (N_L) Values of Human Red Blood Cells

	Red blood cells			Sickle cells		
Counts/300 sec	Frequency	Relative frequency	Percentage of N_L values	Frequency	Relative frequency	Percentage of N_L values
175-199	1	0.0033	0.33	1	0.0333	3.33
200-224	1	0.0033	0.33			
225-249	16	0.0533	5.33	3	0.1000	10.00
250-274	20	0.0666	6.66	4	0.1333	13.33
275-299	33	0.1100	11.00	4	0.1334	13.34
300-324	39	0.1300	13.00	6	0.2000	20.00
325-349	41	0.1376	13.76	2	0.0667	6.67
350-374	36	0.1200	12.00	2	0.0667	6.67
375-399	28	0.0933	9.33	2	0.0667	6.67
400-424	28	0.0933	9.33	2	0.0667	6.67
425-449	19	0.0633	6.33			
450-474	12	0.0400	4.00	1	0.0333	3.33
475-499	7	0.0233	2.33	1	0.0333	3.33
500-524	4	0.0133	1.33			
525-449	9	0.0300	3.00	1	0.0333	3.33
550-574						
575-599	1	0.0033	0.33			
600-624	1	0.0033	0.33	1	0.0333	3.33
625-649						
650-674	2	0.0066	0.66			
675-699	1	0.0033	0.33			
700-724						
> 1000	1	0.0033	0.33			
	300	1.0000	100.00	30	1.0000	100.00

Table VIII

Total Intensity (N_T) Values for Fe K_a in Euhemic Cells on Quartz

	Mean	SD	V	$(SD)^2$
Cell	3395	132	3.89	17,424
	3249	145	4.46	21,025
	4012	121	1.06	14,641
	3935	47	1.19	2,209
	3836	150	3.91	22,500
	3844	136	1.54	18,496
	3885	2213	56.96	4,897,369
	2178	1777	81.59	3,157,729
	1493	73	4.89	5,329
	2530	2150	84.98	4,622,500
	----	----	-----	---------
	3236	694	21.46	482,191
Support	3708	230	6.20	52,900
	3627	107	2.95	11,449
	4220	139	3.29	19,321
	4147	53	1.28	2,809
	4044	142	3.51	20,164
	4200	84	2.00	7,056
	3840	2136	55.62	4,562,496
	2304	1957	84.94	3,829,849
	1495	50	3.34	2,500
	2450	1942	79.27	3,771,364
	----	----	-----	---------
	3403	684	20.09	467,856

Table IX

Total Intensity (N_T) Values for Fe K_a in Red Cells from Sickle Cell Anemia Patients on Quartz

	Mean	SD	V	$(SD)^2$
Cell	3636	1399	38.48	1,957,201
	1292	37	2.86	1,369
Sickle	1254	65	5.18	4,225
	1239	47	3.79	2,209
	1310	80	6.11	6,400
	1213	43	3.54	1,849
	1657	278	9.99	328,875
Normal appearing	3633	1677	46.16	2,812,329
	1368	43	3.14	1,849
	1223	36	2.94	1,296
	1229	69	5.61	4,761
	1304	67	5.14	4,489
	1242	52	4.19	2,704
	1666	324	11.20	471,238
	1661	201	10.59	400,056
Support	3370	1400	41.54	1,960,000
	1485	59	3.97	3,481
	1415	68	4.81	4,624
	1365	48	3.52	2,304
	2061	1476	71.62	2,178,576
	1375	77	5.60	5,929
	1845	521	21.84	692,486

Table X

Intensity Values for Fe K_a of Euhemic Cells on Thin Film

	N_T	N_B	N_L	N_T/N_B
Cell	574	393	181	1.46
	2370	1977	393	1.20
	799	623	176	1.28
	766	588	178	1.30
	869	605	264	1.44
	836	571	265	1.46
	803	536	267	1.50
	766	499	267	1.54
	---	---	---	---
	973	724	249	1.40

Table XI

Fe K_a Intensity Values Comparison, EMPA and SEM-EDX

Iron K_a X-radiation				
		EMPA	SEM-EDX	
Cell type	*	Quartz	Thin film	Quartz
Euhemic	N_T	147 21 ± 0.2	973 571 ± 71	3236 694 ± 69
	N_B	68	724	2902
	N_L	79	249	291
	MDL	0.1%	0.1%	0.2%
	P/B	2.2	1.3	1.1
			Quartz	
			Sickle	Normal appearing
Sickle	N_T	132 18 ± 0.6	1657 278 ± 46	1666 324 ± 54
	N_B	64	1486	1548
	N_L	68	118	100
	MDL	0.1%	0.3%	0.4%
	P/B	2.1	1.1	1.1

*Legend:
Total counting peak: N_T counts
Background: N_B counts
Net count in peak: N_L counts
MDL (wt%) 60 sec: MDL
P/B ("Gross peak"-to-Bkgd ratio): N_T/N_B

FIGURE CAPTIONS

Fig. 1. Diagram of reference standard preparation: pelleted human hemoglobin and human serum albumin on support.

Fig. 2a. Scanning electron micrograph of whole blood smear, air-dried and carbon coated. X500. Acceleration voltage 10 keV, beam diameter 200 nm, beam current 100 μA, scan exposure rate 40 sec.

Fig. 2b. Scanning electron micrograph of an air-dried whole blood smear. X2,000. Acceleration voltage 10 keV, beam diameter 200 nm, beam current 100 μA, scan exposure rate 40 sec.

Fig. 2c. Scanning electron micrograph of a freeze-dried whole blood smear. X10,000. Acceleration voltage 5 keV, beam diameter 300 nm, beam current 100 μA, scan exposure rate 40 sec.

Fig. 3. Scanning electron micrograph shows images of euhemic human red blood cells mounted on thin film (Formvar). These cells are fixed-washed, then mounted, air dried, and examined without any coating of conductive material. X4,000. Acceleration voltage 10 keV, beam diameter 200 nm, beam current 100 μA, scan exposure rate 40 sec.

Fig. 4. Scanning electron micrographs illustrate the technique of stereo-pairs in the SEM as displayed vertically rather than the usual horizontal parallel pairing arrangement. X500. Operating conditions same as Fig. 3.

Fig. 5. Scanning electron image of the red cell selection procedure using the alphabetized finder grid. X300. Acceleration voltage 10 keV, beam diameter 200 nm, beam current 100 μA, scan exposure rate 40 sec.

Fig. 6. EDX energy spectra of the reference standard. Acceleration voltage 15 keV; beam diameter 200 nm; beam current 100 μA; area scanned: 0.2μ × 0.7μ; T. V. scan rates; integration time 1,000 sec.

Fig. 7. EDX energy spectra of a single human rbc mounted on SiO_2. Compare Fig. 8. Acceleration voltage 15 keV; beam diameter 200 nm; beam current 100 μA; area scanned: 0.2μ × 0.7μ; T. V. scan rates; integration time 1,000 sec.

Fig. 8. EDX energy spectra of a single human rbc mounted on thin film (Formvar). Acceleration voltage 15 keV; beam diameter 200 nm; beam current 100 μA; area scanned: 0.2μ × 0.7μ; T. V. scan rates; integration time 1,000 sec.

Fig. 9. A representation of an Fe K_a energy spectrum removed from a typical EDX spectra plot. Integration time: five 1-minute scans at T. V. rates; analyses: on and off cell; cell mounts: quartz disks and thin film (Formvar).

Fig. 10. Histogram of results for quantitative analysis (EMPA) using data from Table VII. Relative net iron K-radiation distributions are given.

Fig. 11a. Scanning electron image of a euhemic human red blood cell. The biconcave, rounded shape in appearance is observable. X5,000. Acceleration voltage 10 keV, beam diameter 20 nm, beam current 100 μA, scan exposure rate 70 sec.

Fig. 11b. Scanning electron image of a euhemic red blood cell. Though biconcave, rounded appearance is yet observable, some flattening, too, is in evidence. X5,000. Acceleration voltage 10 keV, beam diameter 20 nm, beam current 100 μA, scan exposure rate 70 sec.

Fig. 12. Scanning electron images of sickle cells in discocytic and echinocytic forms. X5,000. Acceleration voltage 10 keV, beam diameter 20 nm, beam current 100 μA, scan exposure rate 70 sec.

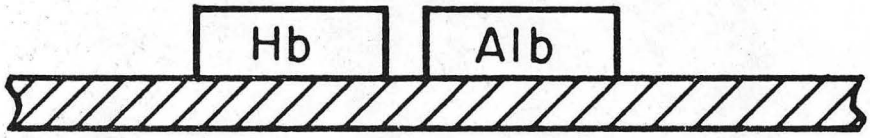

XBL768-9205

Fig. 1 Diagram of reference standard preparation: pelleted human hemoglobin and human serum albumin on support.

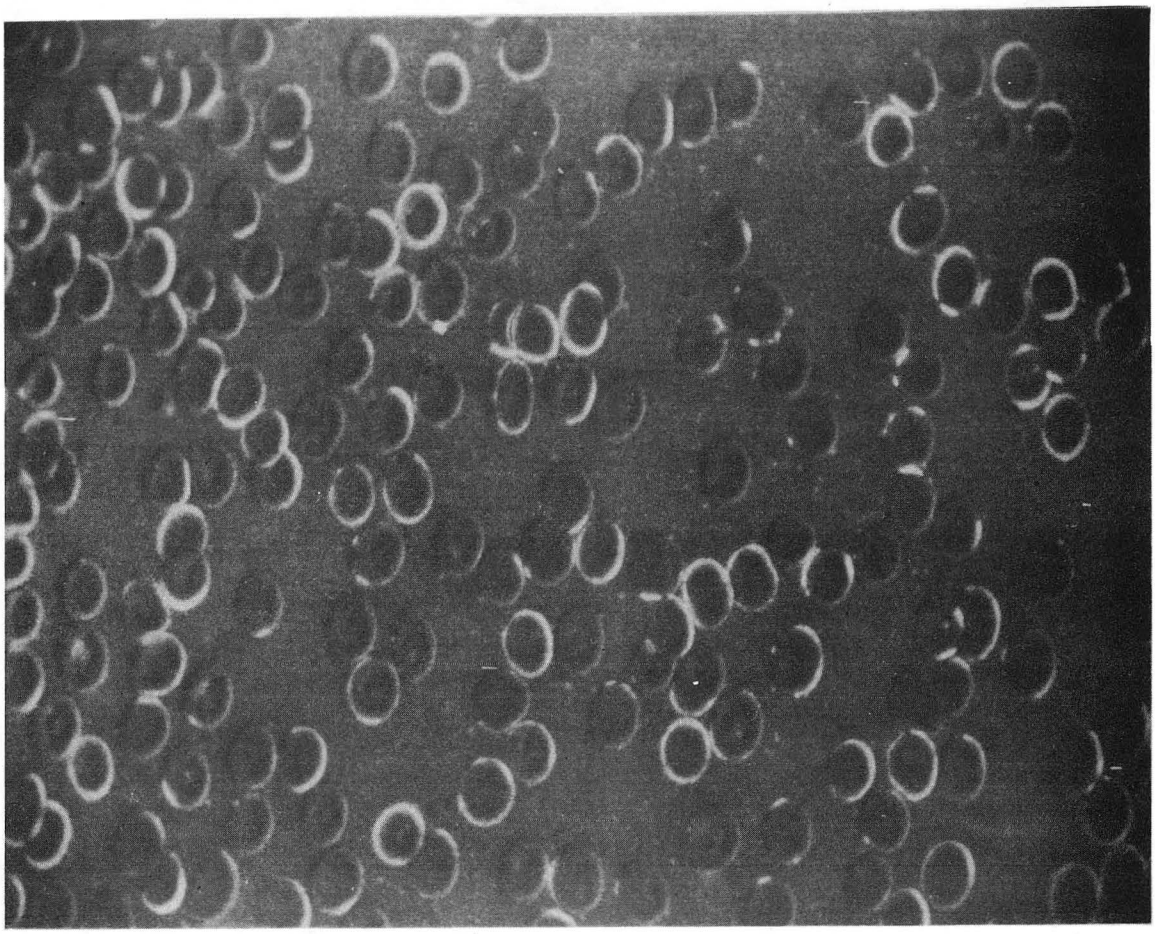

XBB 767-6574

Fig. 2a.

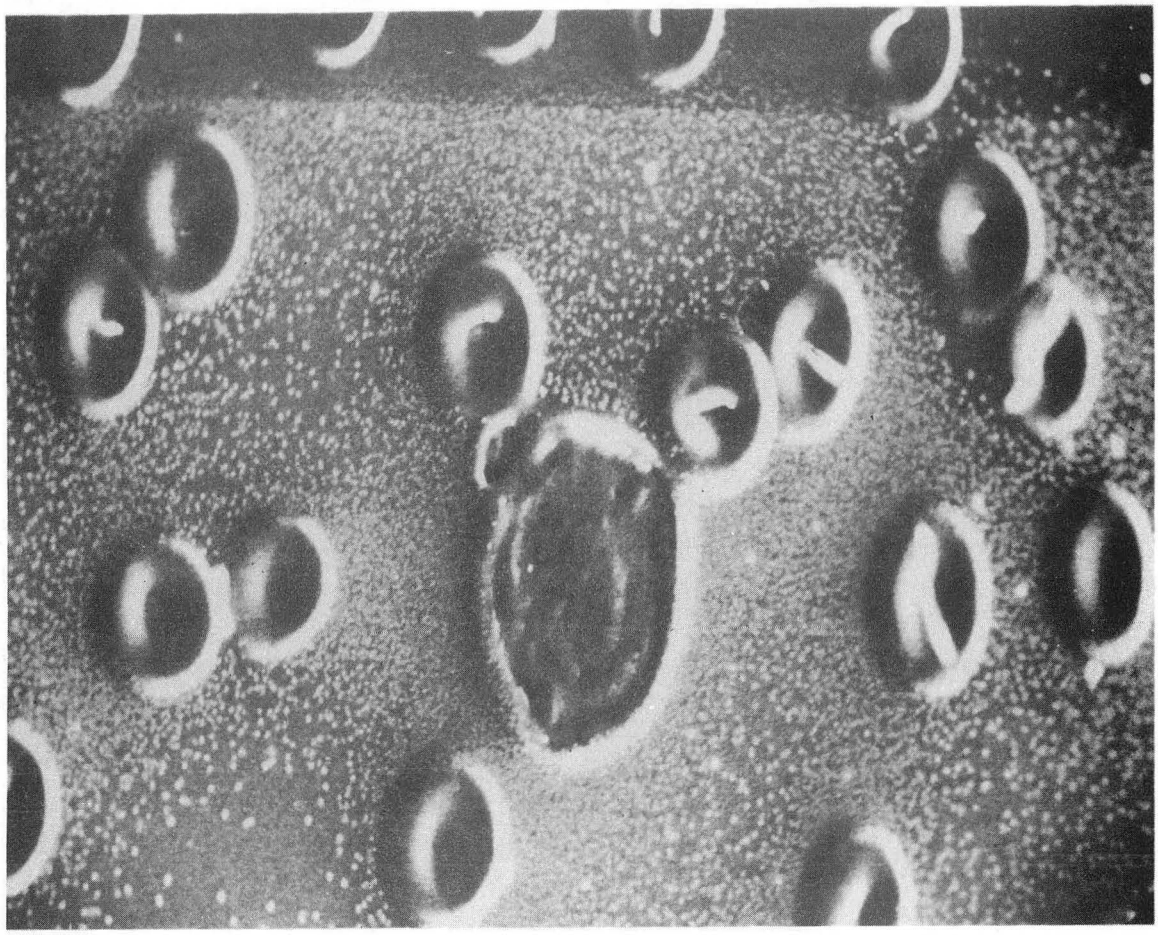

XBB 767-6576

Fig. 2b Scanning electron micrograph of an air-dried whole blood smear. X2,000. Acceleration voltage 10 keV, beam diameter 200 nm, beam current 100 μA, scan exposure rate 40 sec.

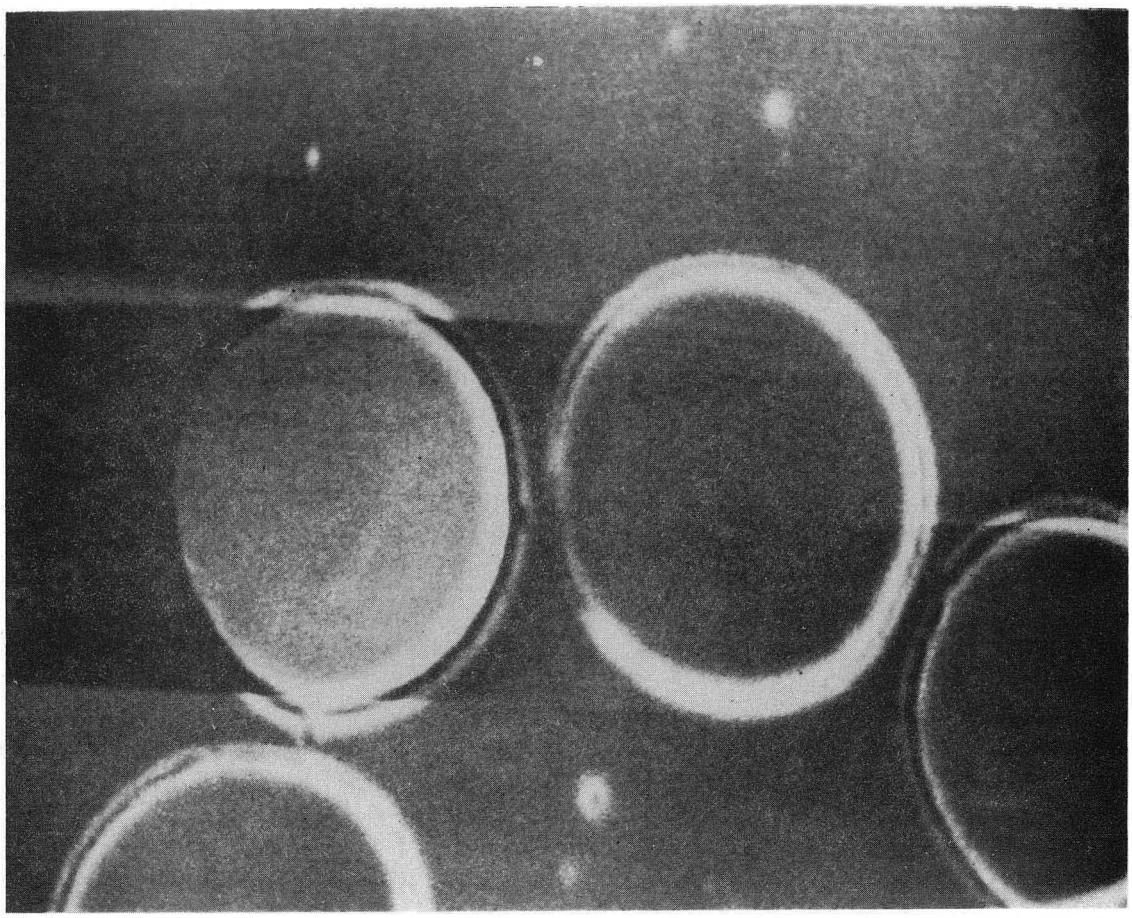

XBB 767-6572

Fig. 2c Scanning electron micrograph of a freeze-dried whole blood smear. X10,000. Acceleration voltage 5 keV, beam diameter 300 nm, beam current 100 μA, scan exposure rate 40 sec.

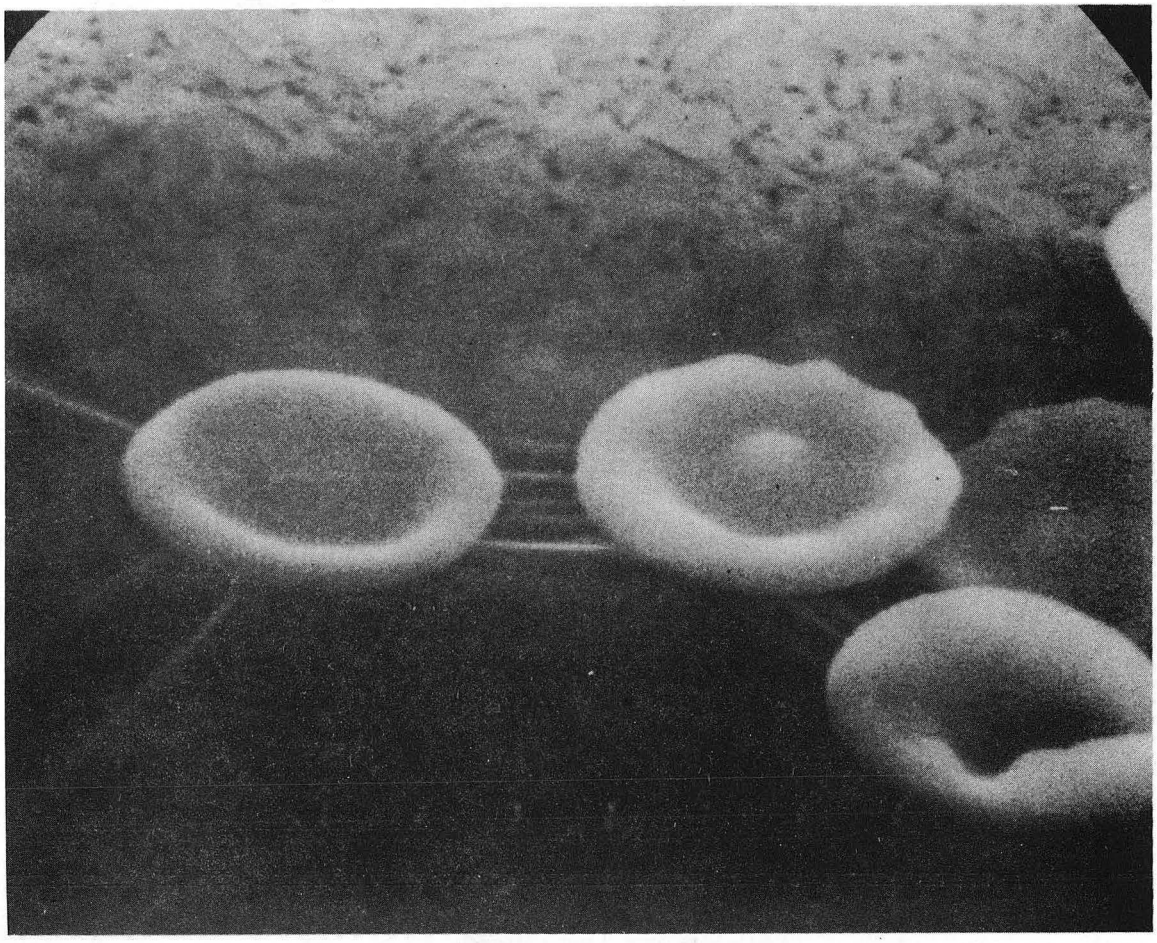

XBB 769-8498

Fig. 3 Scanning electron micrograph shows images of euhemic human red blood cells mounted on thin film (Formvar). These cells are fixed-washed, then mounted, air dried, and examined without any coating of conductive material. X4,000. Acceleration voltage 10 keV, beam diameter 200 nm, beam current 100 μA, scan exposure rate 40 sec.

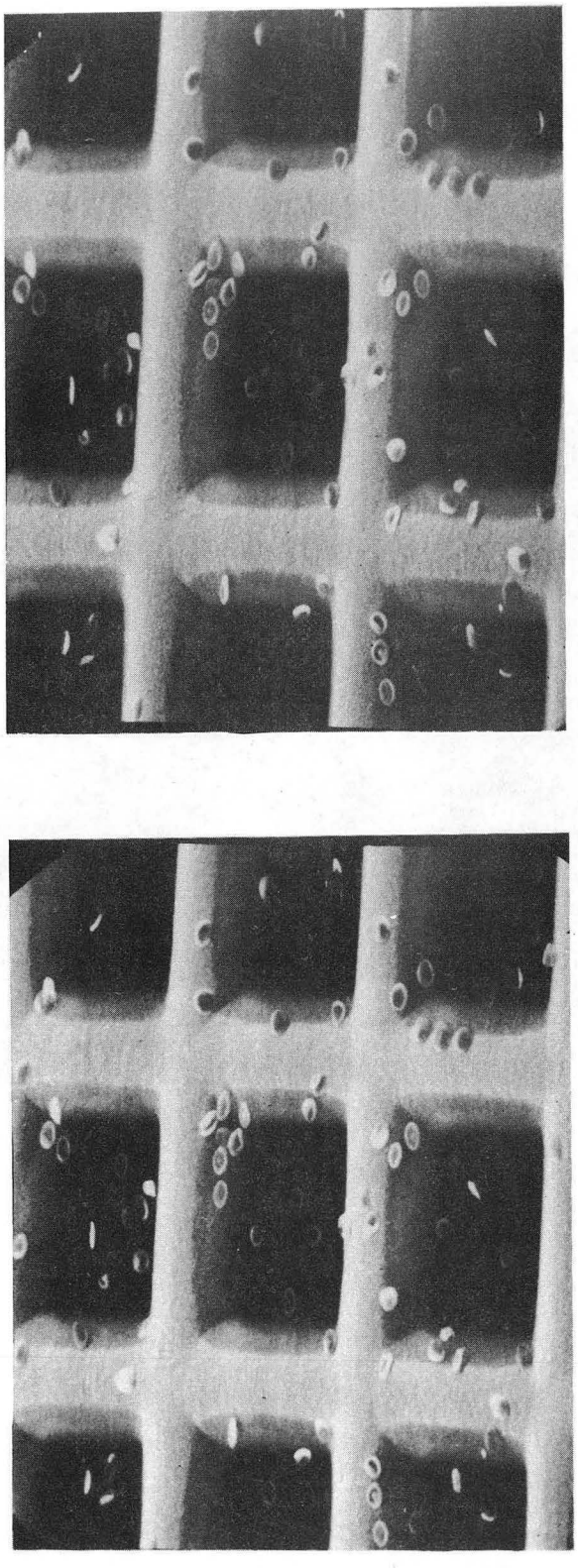

XBB 7610-9356

Fig. 4 Scanning electron micrographs illustrate the technique of stereopairs in the SEM as displayed vertically rather than the usual horizontal parallel pairing arrangement. X500. Operating conditions same as Fig. 3.

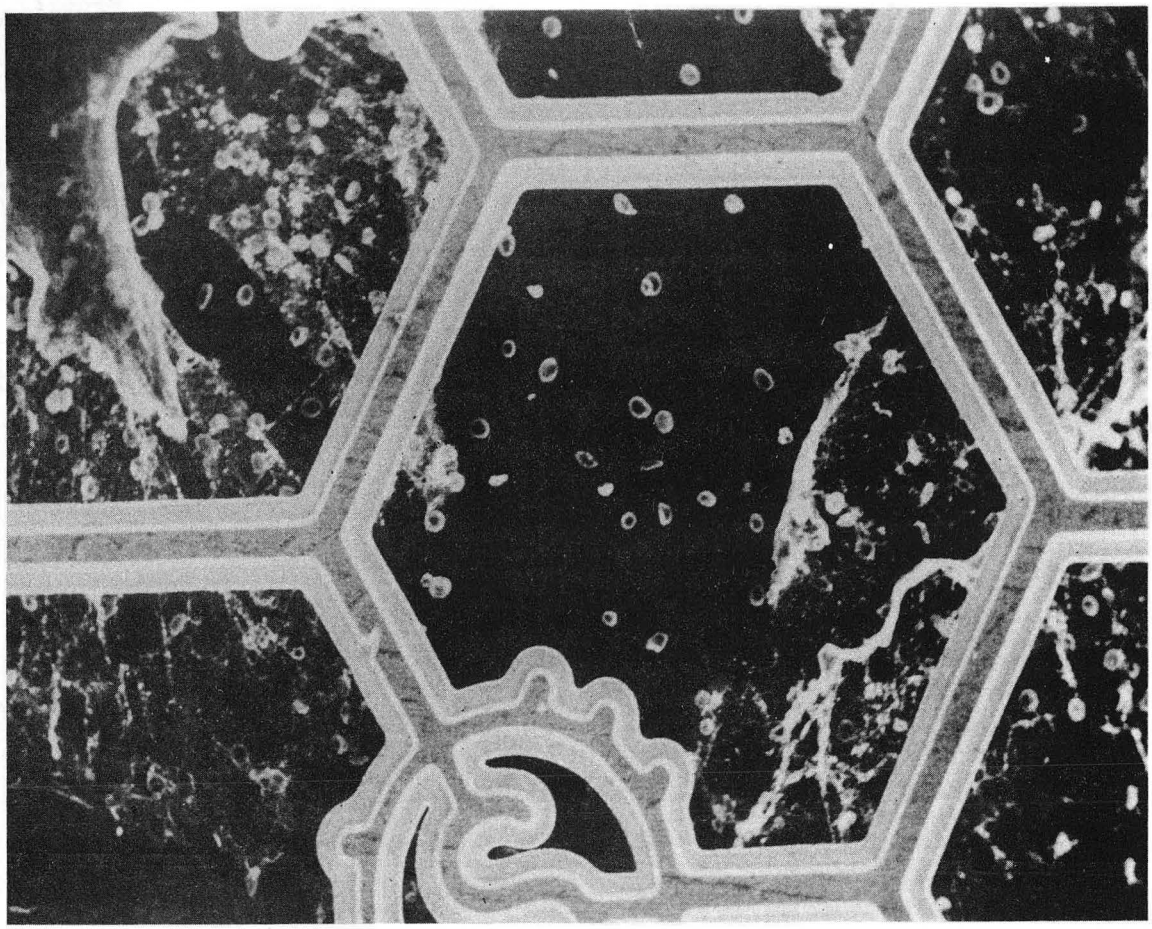

XBB 767-6567

Fig. 5 Scanning electron image of the red cell selection procedure using the alphabetized finder grid. X300. Acceleration voltage 10 keV, beam diameter 200 nm, beam current 100 μA, scan exposure rate 40 sec.

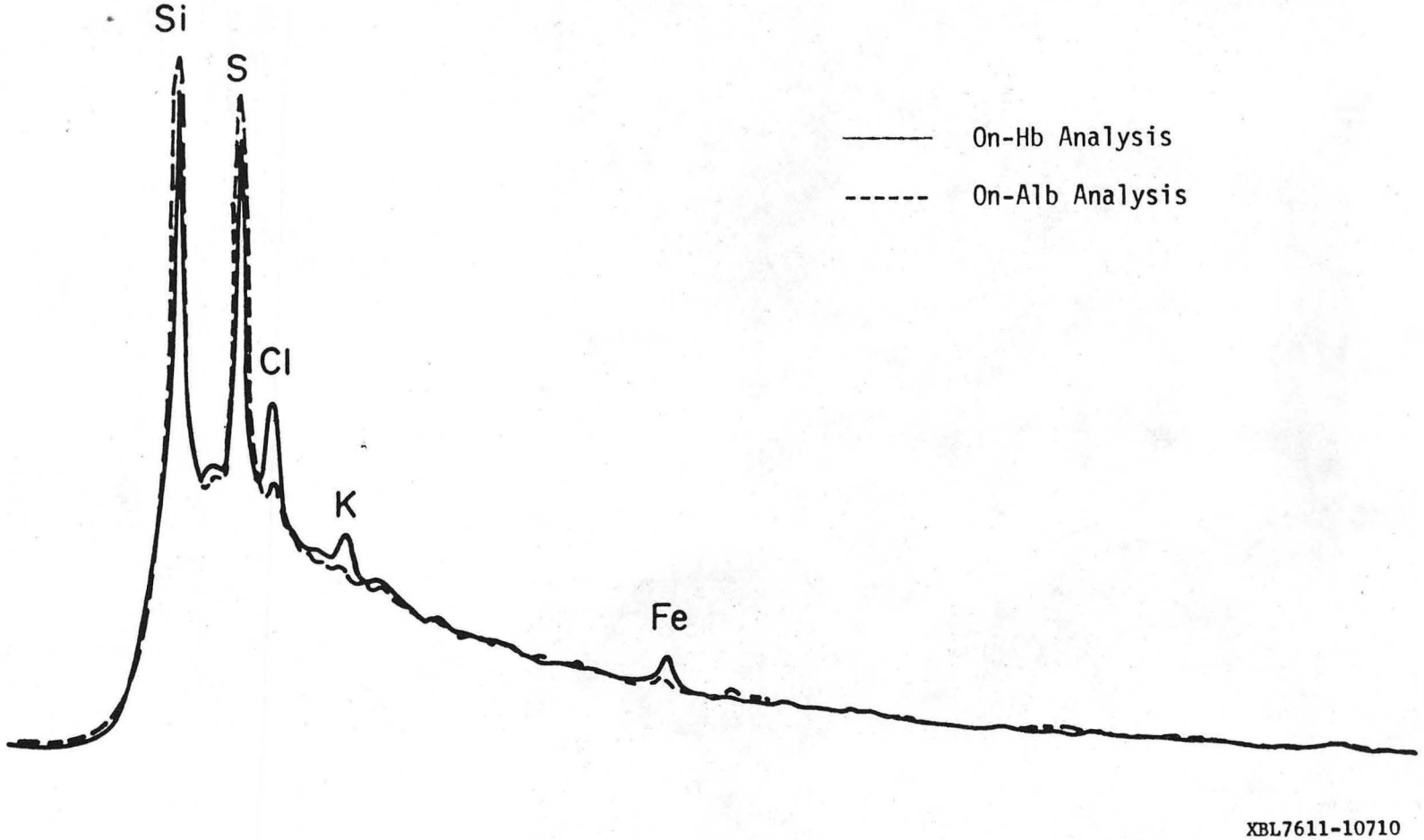

Fig. 6 EDX energy spectra of the reference standard. Acceleration voltage 15 keV; beam diameter 200 nm; beam current 100 μA; area scanned: 0.2μ × 0.7μ; T. V. scan rates; integration time 1,000 sec.

Fig. 7 EDX energy spectra of a single human rbc mounted on SiO_2. Compare Fig. 8. Acceleration voltage 15 keV; beam diameter 200 nm; beam current 100 μA; area scanned: 0.2μ × 0.7μ; T. V. scan rates; integration time 1,000 sec.

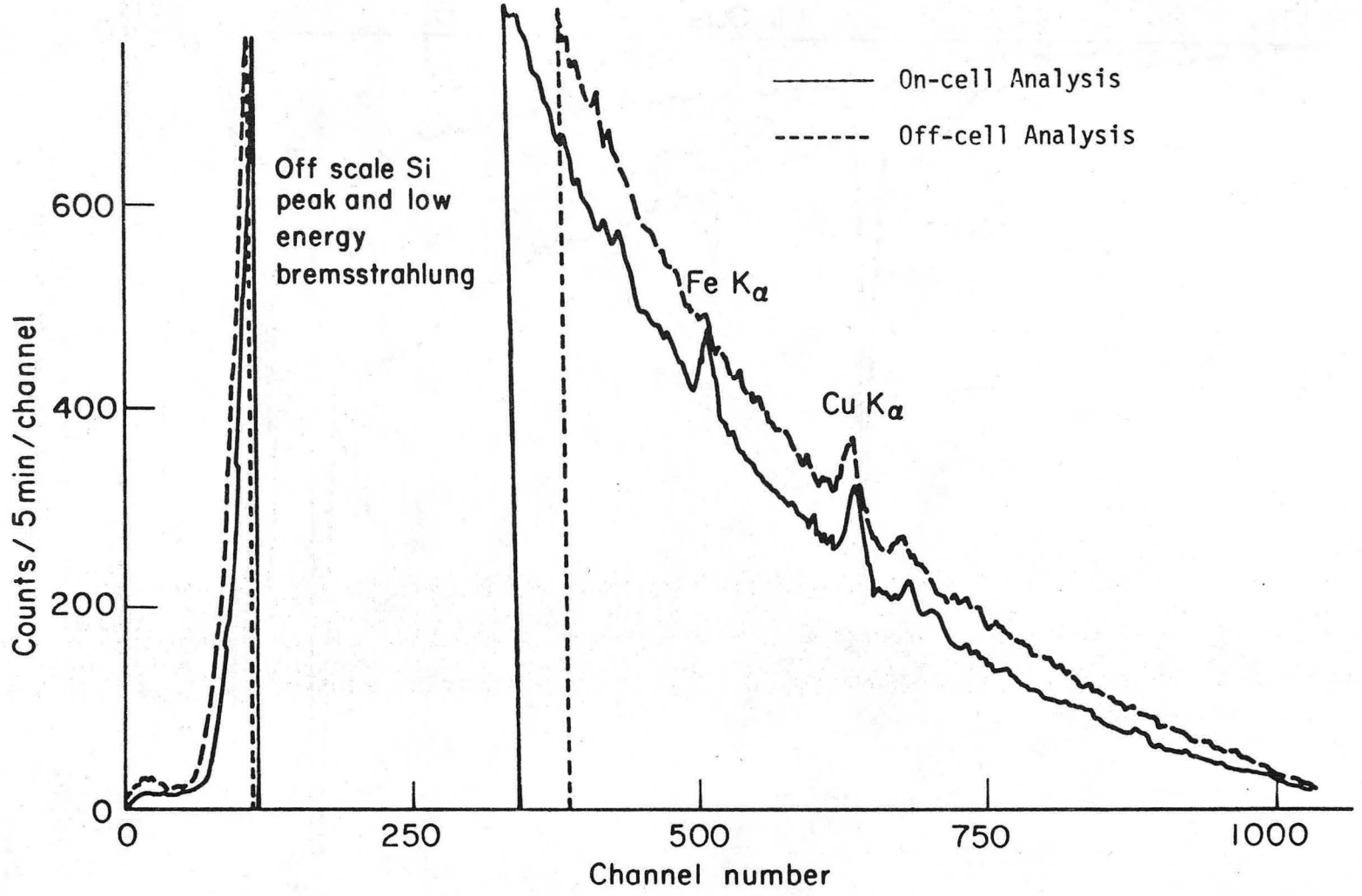

XBL7610-9360

Fig. 8 EDX energy spectra of a single human rbc mounted on thin film (Formvar). Acceleration voltage 15 keV; beam diameter 200 nm; beam current 100 μA; area scanned: 0.2μ × 0.7μ; T. B. scan rates; integration time 1,000 sec.

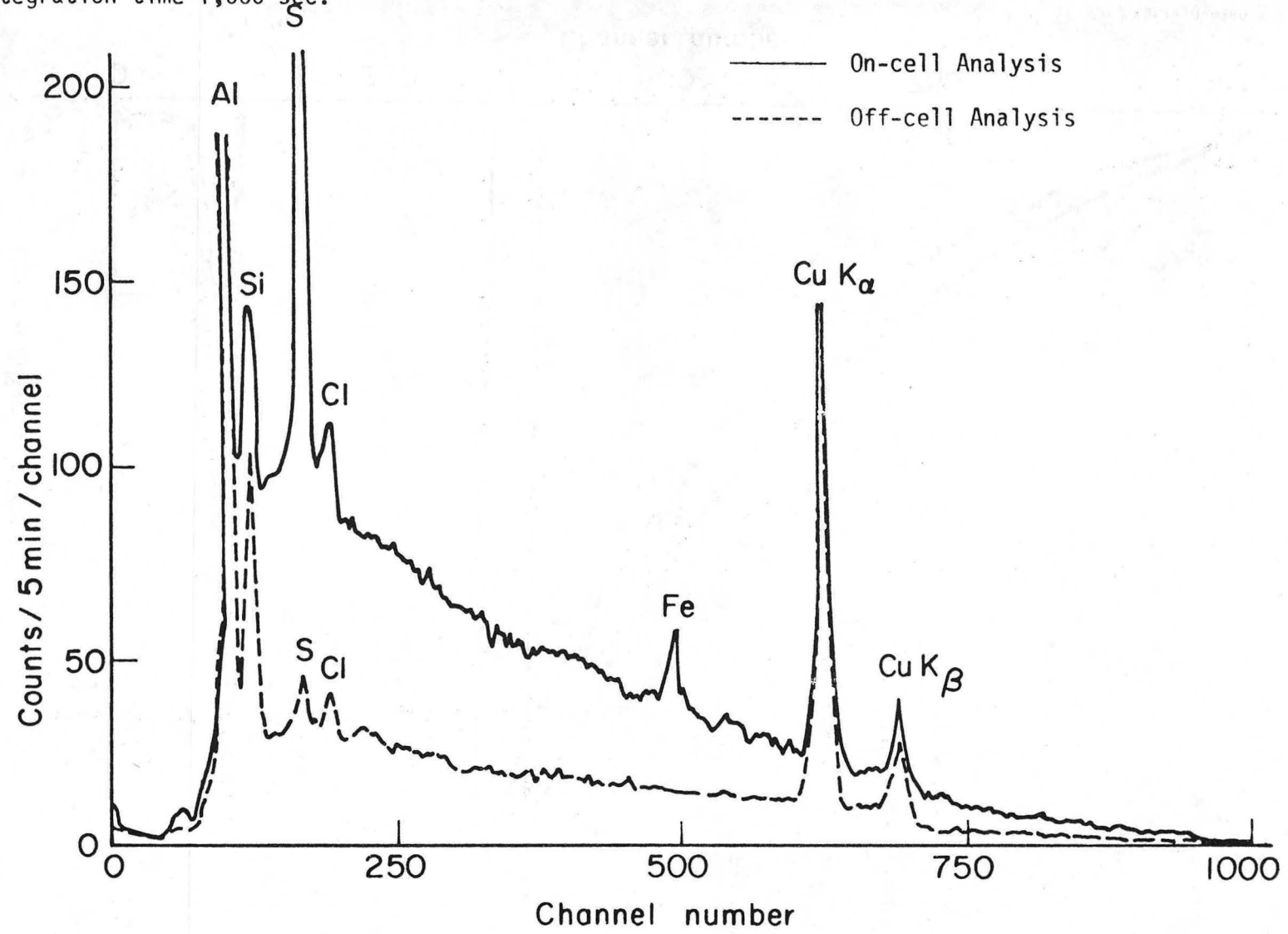

XBL 769-10655

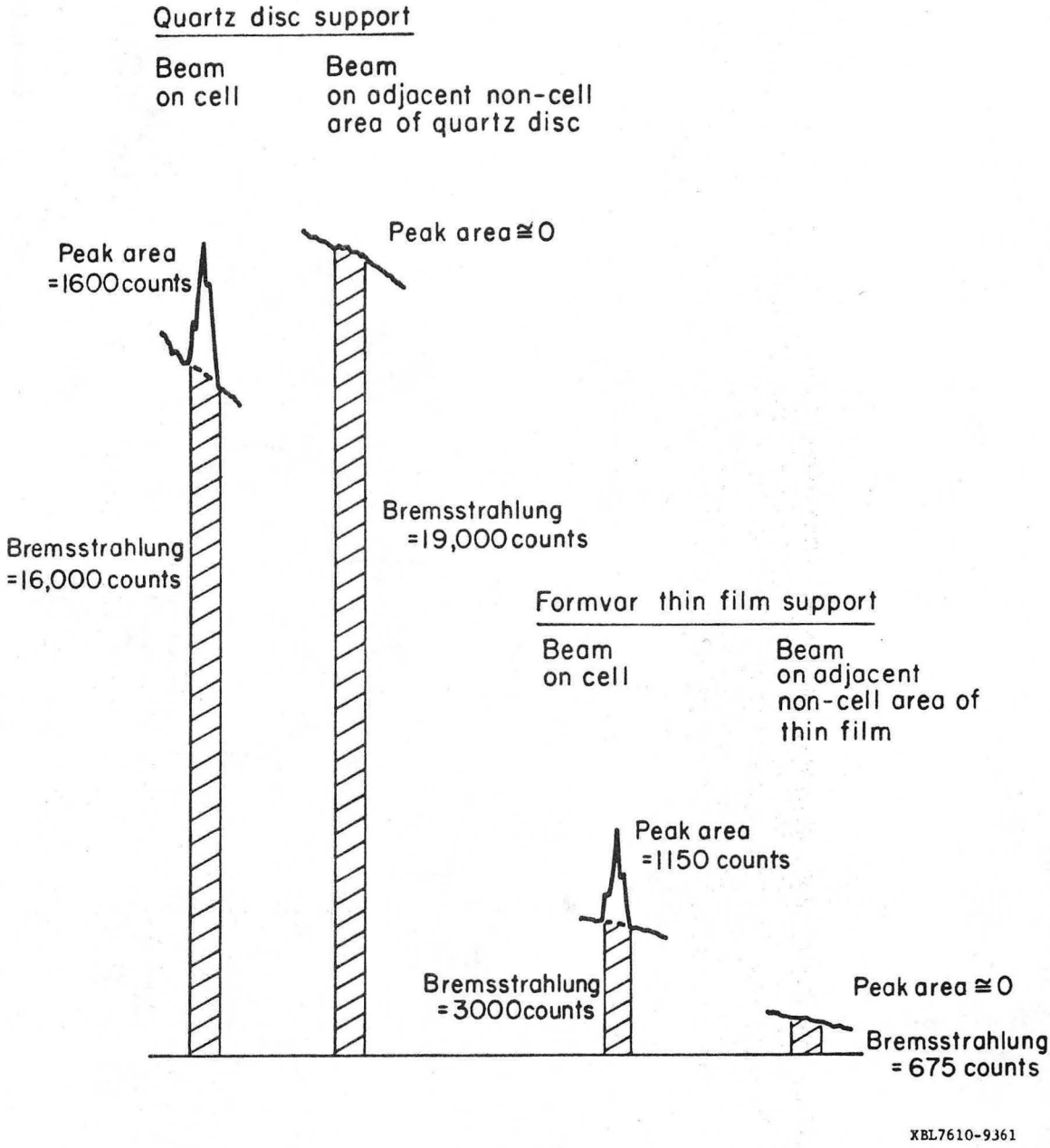

Fig. 9 A representation of an Fe K_a energy spectrum removed from a typical EDX spectra plot. Integration time: five 1-minute scans at T. V. rates; analyses: on- and off-cell; cell mounts: quartz disks and thin film (Formvar).

Fig. 10 Histogram of results for quantitative analysis (EMPA) using data from Table VII. Relative net iron K-radiation distributions are given.

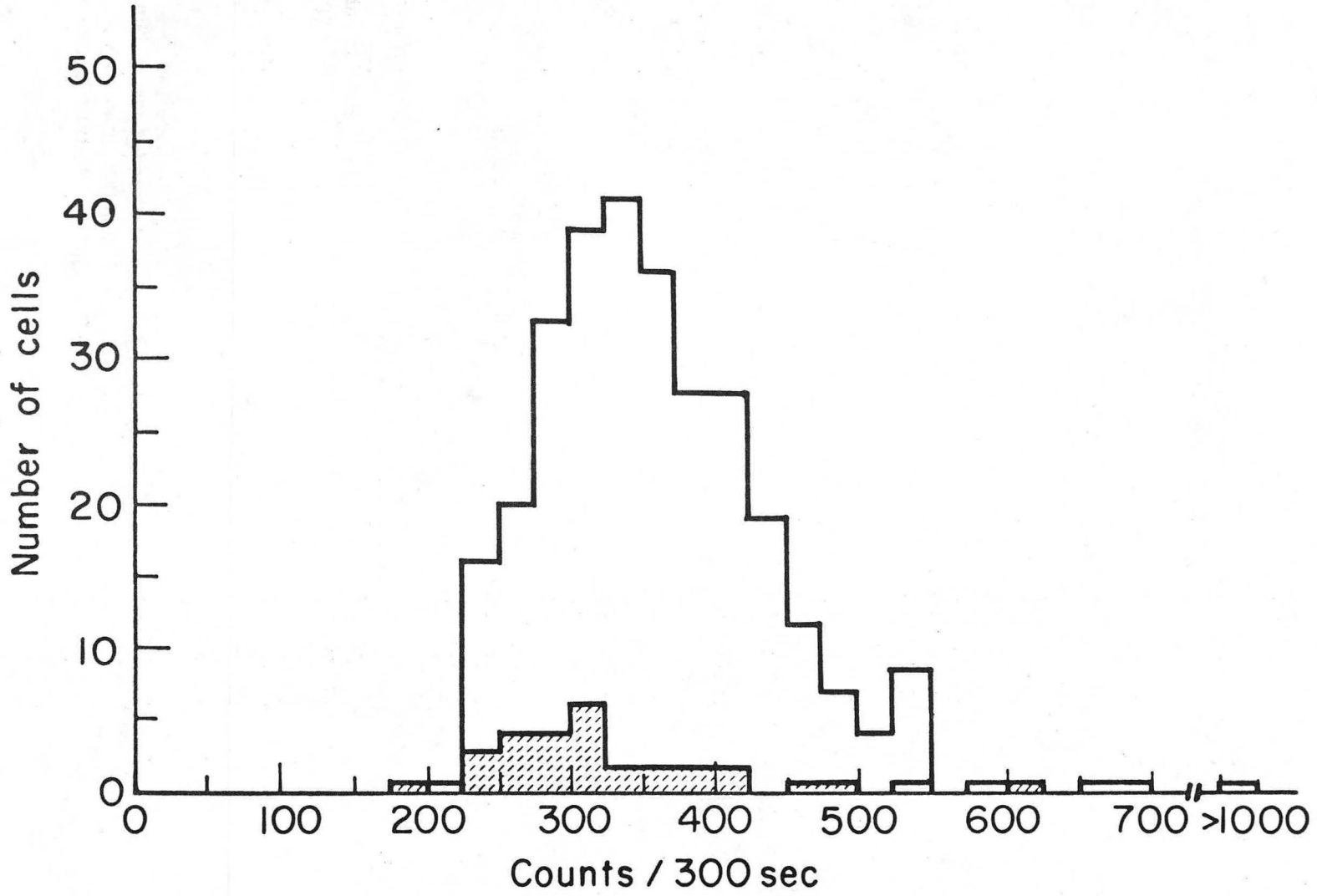

XBL 769-10656

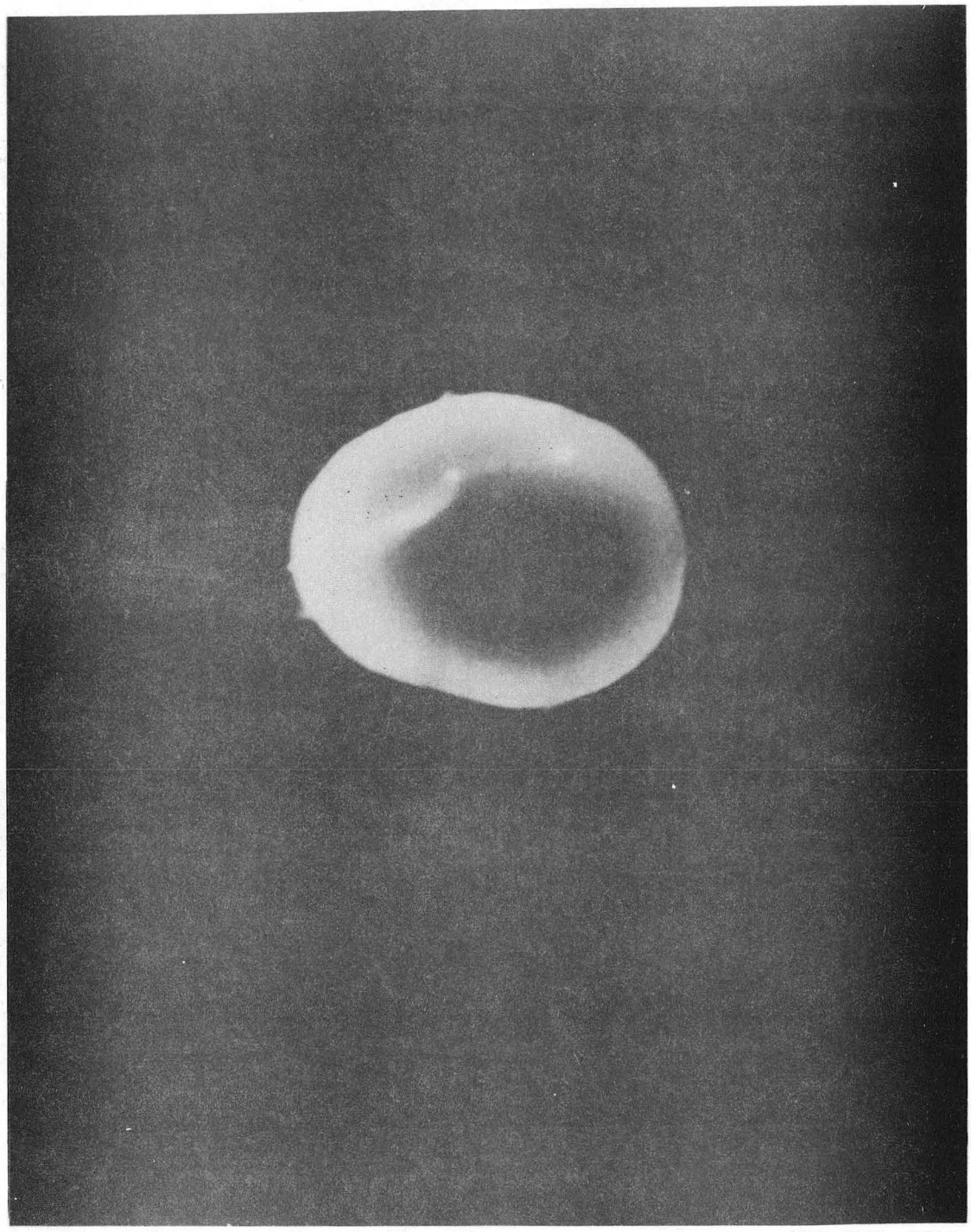

XBB 768-6876

Fig. 11a Scanning electron image of a euhemic human red blood cell. The biconcave, rounded shape in appearance is observable. X5,000. Acceleration voltage 10 keV, beam diameter 20 nm, beam current 100 μA, scan exposure rate 70 sec.

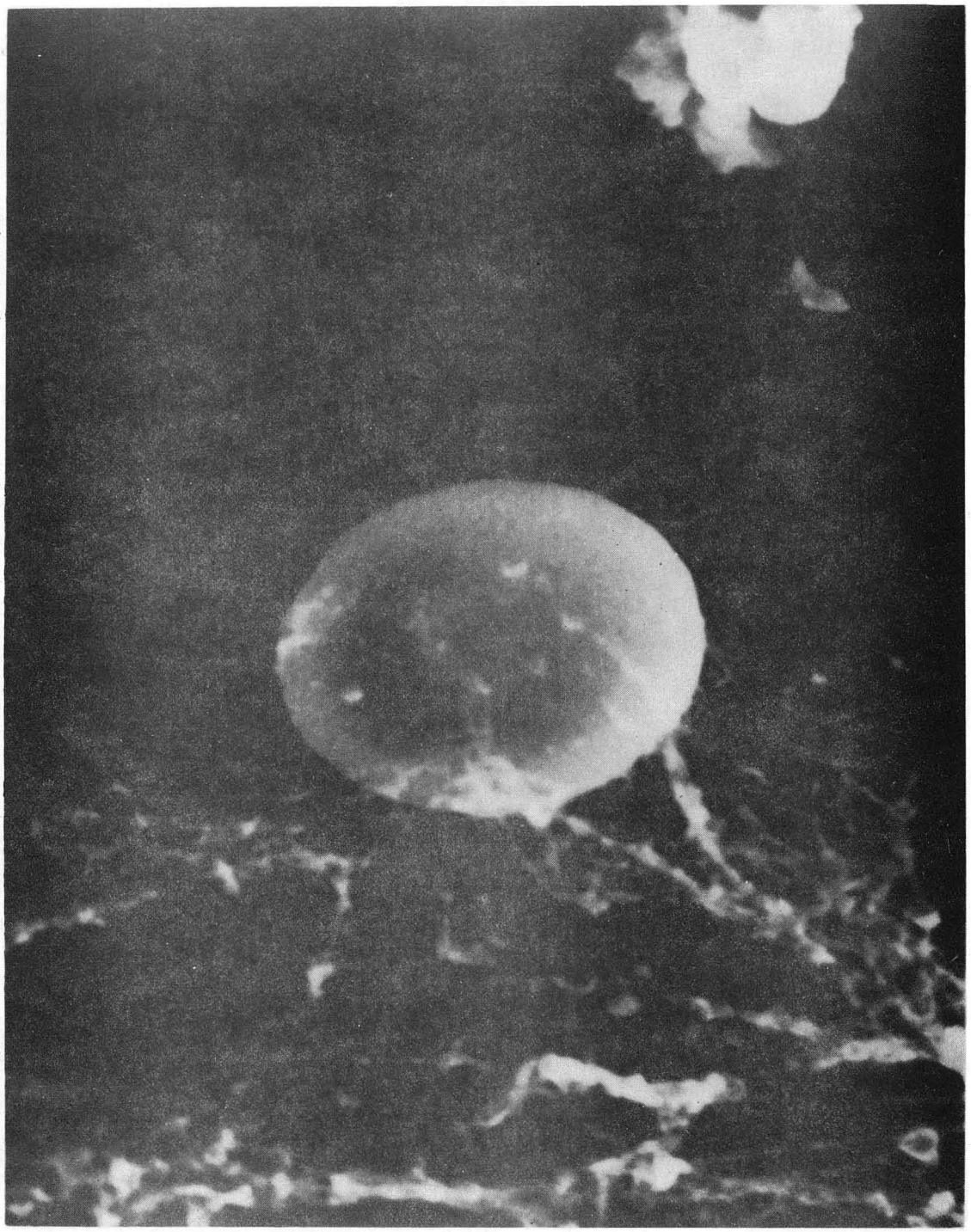

XBB 768-6875

Fig. 11b Scanning electron image of a euhemic human red blood cell. Though biconcave, rounded appearance is yet observable, some flattening, too, is in evidence. X5,000. Acceleration voltage 10 keV, beam diameter 20 nm, beam current 100 μA, scan exposure rate 70 sec.

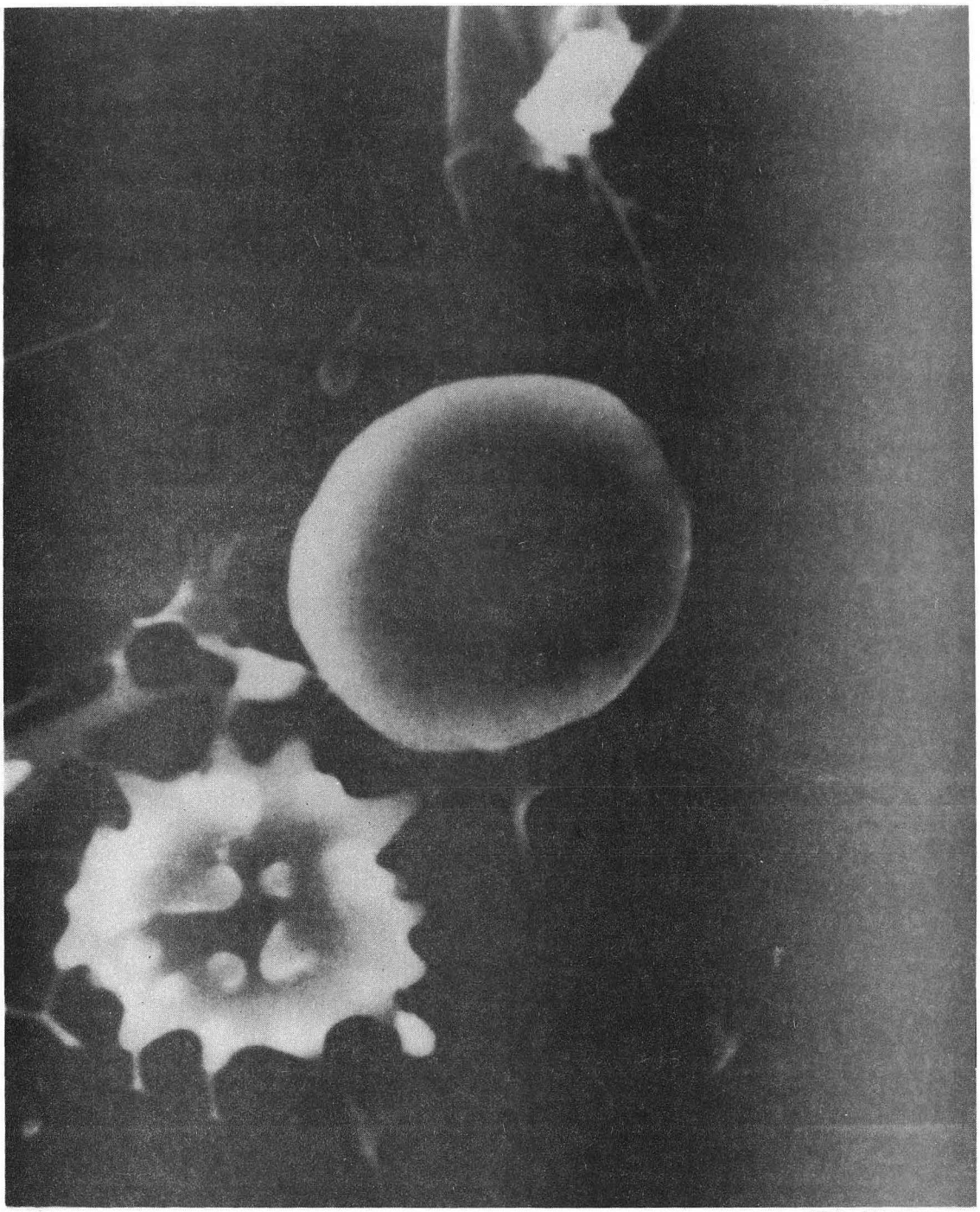

XBB 767-6577

Fig. 12 Scanning electron images of sickle cells in discocytic and echinocytic forms. X5,000. Acceleration voltage 10 keV, beam diameter 20 nm, beam current 100 μA, scan exposure rate 70 sec.

TECHNICAL INFORMATION DEPARTMENT
LAWRENCE BERKELEY LABORATORY
UNIVERSITY OF CALIFORNIA
BERKELEY, CALIFORNIA 94720